Rev. Roum. Sci. Techn.– Électrotechn. et Énerg.
Vol. **70**, *3*, pp. 349–354, Bucarest, 2025

A NOVEL PROTOTYPING APPROACH TO BROADBAND MICROSTRIP 90 DEGREES PHASE SHIFTERS

LAURENȚIU IUSTIN BUZINCU[1], IOAN NICOLAESCU[2]

Keywords: Microwave phase shifters; Prototyping; C-section; Microstrip coupled lines; Impedance matrix; Genetic algorithm; Schiffman phase shifter.

This work presents a series of computer modeling experiments conducted to streamline the synthesis of a family of broadband microwave 90-degree phase shifters. While most broadband microwave phase shifters based on segments of coupled transmission lines were initially designed with symmetric transmission lines, current approaches require adapting such designs to microstrip lines. The proposed approach involves the development of simple mathematical models for three representative 90-degree phase shifters and the application of available MATLAB genetic optimization algorithms to synthesize the microstrip lines incorporated into the phase shifters. The results are validated by implementing the synthesized circuit in Ansys CIRCUIT and further improved by developing and optimizing more detailed models in Ansys HFSS.

1. INTRODUCTION

The synthesis of 90-degree microwave phase shifters based on coupled lines, capable of providing a roughly constant phase shift over a wide bandwidth, has been a subject of interest for decades. While most of the original topologies and synthesis methods found in the literature are based on coupled striplines, practical considerations require the transition of such designs to microstrip (MIC) coupled lines. Since the propagation model in MIC is quasi-TEM, employing MIC lines involves an increased level of complexity in both the analysis and synthesis of the phase shifters. The additional complexity arises from the fact that the propagation velocities of the even and odd modes in MIC coupled lines differ.

In this work, a straightforward and simplified approach to synthesizing broadband phase shifters is proposed. To demonstrate the design strategy, it was applied to the following known phase shifters: the classical "Type A" phase shifter as Schiffman introduced it [2] which, from this point on, will be called the Schiffman Phase Shifter (SPS); the basic design of a matched broadband phase shifter as proposed by Schiek, et. al. [3] which, for brevity, will be called herein the Schiek Phase Shifter (SKPS); and, the ultra-wideband phase shifter based on a short circuit stub and weak coupled lines proposed by Liu, et. al. [4] which will be called the Liu Phase Shifter (LPS). Thus, the advantages and drawbacks of each phase shifter design could be thoroughly compared with the information available in the literature. It is worthwhile to note that the central issue of interest in this investigation was to obtain a phase shifter capable of providing good impedance matching within a bandwidth comparable to that where the constant phase condition is fulfilled. In addition, employing MATLAB codes for analyzing and synthesizing microwave circuits is highly productive [5], provided the mathematical models that the coding is based on are sound.

There were four steps which proved instrumental in implementing the proposed synthesis approach: (1) building a simple yet precise mathematical model of the chosen phase shifter design; (2) identifying a precise enough set of formulas for modeling the parameters of the coupled/ singular MIC lines employed in the construction of the phase shifter; to simplify the modelling of the transmission lines, the decision was made to ignore the losses; (3) coding the relations developed/ identified during the previous two steps into a MATLAB library; (4) synthetizing the dimensions of the elements included in the circuitry of the phase shifter in accordance with the objectives of the design. The synthesis was implemented by adapting the Genetic Algorithm included in the MATLAB Library to the task at hand. The resulting sizes of the MIC lines were further introduced into the MATLAB models of the phase shifters to verify whether the required performance was fulfilled. Additionally, a cross-check of the results was performed by building Ansys CIRCUIT and HFSS models. Thus, the results of the Ansys simulations were compared with the results of the simulations provided by the MATLAB model.

The main goals of the investigation summarized above were, on the one hand, to make available a phase shifter design tool and, on the other hand, to provide an alternative course of action for designers of various MIC circuits that can be adapted to the procedure presented herein.

2. DEVELOPING PHASE SHIFTERS' MATHEMATICAL MODELS

As the mathematical models were developed for phase shifters employing MIC coupled lines, the first step in modeling was defining the mathematical model of the coupled lines themselves. The chosen approach was a straightforward generalization of the coupled lines' impedance matrix as described by Jones and Bolljahn in [1]. Thus, a pair of coupled MIC lines can be represented as a four-port, and the elements of the impedance matrix are shown below:

$$Z_{11} = Z_{22} = Z_{33} = Z_{44} = -j\left(Z_e \frac{\cot\theta_e}{2} + Z_o \frac{\cot\theta_o}{2}\right). \quad (1)$$

$$Z_{12} = Z_{21} = Z_{34} = Z_{43} = -j\left(Z_e \frac{\cot\theta_e}{2} - Z_o \frac{\cot\theta_o}{2}\right). \quad (2)$$

$$Z_{13} = Z_{31} = Z_{24} = Z_{42} = -j\left(Z_e \frac{\csc\theta_e}{2} - Z_o \frac{\csc\theta_o}{2}\right). \quad (3)$$

$$Z_{14} = Z_{41} = Z_{23} = Z_{32} = -j\left(Z_e \frac{\csc\theta_e}{2} + Z_o \frac{\csc\theta_o}{2}\right). \quad (4)$$

where Z_{ij} are the elements of the 4 by 4 impedance matrix, Z_e and Z_o are the even mode and the odd mode characteristic impedances, while θ_e and θ_o are the even and odd mode phase shifts introduced by the coupled lines. The equations given in [7]-[12] were later employed to calculate the elements of the impedance matrix. Starting from the basic

[1] Military Technical Academy, Ferdinand I, Bucharest, Romania.
E-mails: laurentiu.buzincu@mta.ro, ioan.nicolaescu@mta.ro

DOI: 10.59277/RRST-EE.2025.70.3.11

representation shown above, the models for the three phase shifters identified in the previous section are deduced.

In the following, the model of the C-Section that forms the phasing part of the Schiffman Phase Shifter is defined. Of course, the differential phase shifter is composed of the C-Section and includes a MIC reference line, which, due to the simplicity of representation, doesn't need special treatment. The purpose of the further development is to obtain the impedance matrix of the C-Section. The equivalent circuit of the C-Section is shown in Fig. 1. The C-Section model is obtained by interconnecting the ports at one end of the coupled pair. Of course, this interconnection turns the four-port into a two-port. The equivalent impedance matrix of the two-port is obtained by enforcing the appropriate conditions resulting from the interconnection of ports 3 and 4 as shown in Fig. 1.

$$V_3 = V_4. \tag{5}$$

$$I_3 = -I_4. \tag{6}$$

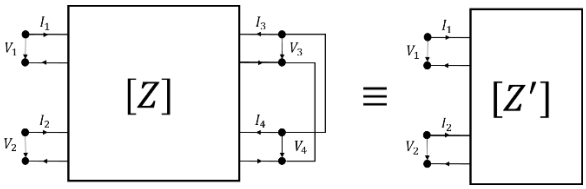

Fig. 1 – C-Section model, Schiffman Phase Shifter.

By simple manipulations of the impedance equations, the symmetrical impedance matrix of the C-Section was obtained, as shown in Equations (7) and (8).

$$Z'_{11} = Z'_{22} = -j\left(Z_e \frac{\cot\theta_e}{2} - Z_o \frac{\tan\theta_o}{2}\right). \tag{7}$$

$$Z'_{12} = Z'_{21} = -j\left(Z_e \frac{\cot\theta_e}{2} + Z_o \frac{\tan\theta_o}{2}\right). \tag{8}$$

The next model was developed for the Schiek Phase Shifter. The topology of the circuit is given in Fig. 2.

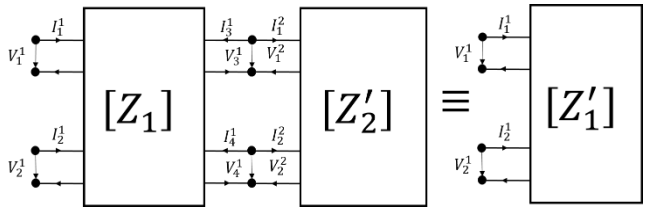

Fig. 2 – Modified C-Section model, Schiek Phase Shifter.

As stated in Introduction, a simple model of phase shifter was chosen where a typical C-Section, with the impedance matrix Z'_2 was connected to a regular coupled-line pair with the impedance matrix Z_1. The impedance matrix of the equivalent two-port circuit is Z'_1. To calculate the impedance matrix mentioned, the following relations among currents and voltages had to be enforced:

$$I_3^1 = -I_1^2. \tag{9}$$

$$I_4^1 = -I_2^2. \tag{10}$$

$$V_3^1 = V_1^2. \tag{11}$$

$$V_4^1 = V_2^2. \tag{12}$$

By simple manipulations of the relations among voltages and currents, the results presented in equations (13) and (14) were obtained where the impedances Z'_{11_2} and Z'_{12_2} take the same forms as presented in equations (7) and (8), while Z_{11_1}, Z_{12_1}, Z_{13_1}, Z_{14_1} can be calculated from equations (1) to (4). As a conclusion, the values of the impedances are dependent of the physical sizes of the two coupled lined pairs.

$$Z'_{11} = Z_{11_1} + \tag{13}$$

$$+\frac{2Z_{13_1}Z_{14_1}\left(Z'_{12_2}+Z_{12_1}\right)-\left(Z_{13_1}^{\,2}+Z_{14_1}^{\,2}\right)\left(Z'_{11_2}+Z_{11_1}\right)}{\left(Z'_{11_2}+Z_{11_1}\right)^2-\left(Z'_{12_2}+Z_{12_1}\right)^2}$$

$$= Z_{12_1} + \tag{14}$$

$$+\frac{2Z_{13_1}Z_{14_1}\left(Z'_{11_2}+Z_{11_1}\right)-\left(Z_{13_1}^{\,2}+Z_{14_1}^{\,2}\right)\left(Z'_{12_2}+Z_{12_1}\right)}{\left(Z'_{11_2}+Z_{11_1}\right)^2-\left(Z'_{12_2}+Z_{12_1}\right)^2}$$

The third model was developed for the Liu Phase Shifter. From Fig. 3, one can notice that the topology of the LPS includes a C-Section like that of the SPS to which a short-circuited MIC line stub is attached. Note that in Fig. 3 the short-circuited stub is described by the reactive input impedance of the stub (losses ignored): Z_{inSC}.

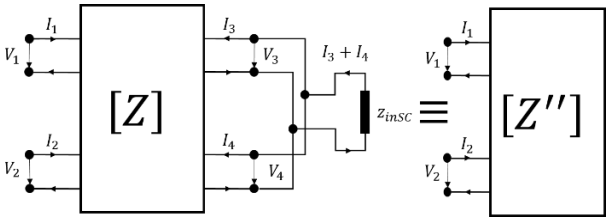

Fig. 3 – Modified C-Section model, Liu Phase Shifter.

While inspecting the topology of the circuit, one can notice that the following equation is valid:

$$V_3 = V_4 = -Z_{inSC}(I_3 + I_4). \tag{15}$$

By inserting (15) into the Z parameter equation relating the currents and voltages associated to the four-port in Fig. 3, the impedance matrix of the equivalent two-port $\mathbf{Z}''$ is extracted. The mentioned matrix is symmetric, and the elements are given below:

$$Z''_{11} = Z_{11} + \tag{16}$$

$$+\frac{2Z_{13}Z_{14}(Z_{inSC}+Z_{12})-(Z_{13}^2+Z_{14}^2)(Z_{inSC}+Z_{11})}{(Z_{11}-Z_{12})(2Z_{inSC}+Z_{11}+Z_{12})}$$

$$Z''_{12} = Z_{12} + \tag{17}$$

$$+\frac{-2Z_{13}Z_{14}(Z_{inSC}+Z_{11})-(Z_{13}^2+Z_{14}^2)(Z_{inSC}+Z_{12})}{(Z_{11}-Z_{12})(2Z_{inSC}+Z_{11}+Z_{12})}$$

where the impedances Z_{ij} are given by equations (1)-(4) while Z_{inSC} can be calculated as the input impedance of a short, circuited MIC line stub.

One can note that any of the phase shifter topologies analyzed above can be logically reduced to a two-port model characterized by a two-by-two symmetrical impedance

matrix. Considering that the ports of the model are connected to 50 Ohm MIC lines, the behavior of the circuit can be easily analyzed by calculating the symmetrical **S** matrix. Thus, S_{11} it will provide information regarding the matching of the circuit while S_{12} providing the information required for assessing the phase shift introduced by the same circuit. The equations employed for calculating the **S** matrices are available in [6].

In addition, under certain circumstances, the evaluation of the image matrix of the two-port circuit might be helpful in synthesis. Therefore, the image matrix of an arbitrary symmetrical two-port characterized by a **Z** matrix is provided below:

$$Z_{image} = \sqrt{Z_{11}^2 - Z_{12}^2}. \quad (18)$$

3. MICROSTRIP LINES EQUATIONS

To evaluate the impedance matrices described in the previous section, a set of equations connecting the dimensions of the lines to their electrical parameters had to be coded. The equations proposed in [7] to [12] were employed to build a MATLAB library that allows for dynamically assessing the electrical parameters of single and coupled lossless MIC lines within the cycles of an optimization algorithm. By inspecting the eq. (1) to (4), it is obvious that there are certain electrical parameters that must be calculated. Thus, MATLAB functions were coded to calculate the even and odd characteristic impedances:

zo_even_dispersion(*eps_rel,t,u,g,z0,fn*). (19)

zo_odd_dispersion(*eps_rel,t,u,g,z0,fn*). (20)

where: *eps_rel* is the dielectric constant of the substrate; *t* is the height of the copper layer normalized to the height of the substrate; *u* is the width of the coupled line normalized to the height of the substrate, *g* is the width of the coupling gap, also normalized to the height of the substrate, *z0* is the wave impedance of vacuum and *fn* is the normalized frequency [10] shown below.

$$f_n = (f/GHz)(h/mm). \quad (21)$$

Also, the functions required to calculate the odd and even mode phase shifts produced by coupled sections were defined:

theta_odd(*eps_rel,u,g,fn,fn_referinta,l,h*). (22)

theta_even(*eps_rel,u,g,fn,fn_referinta,l,h*). (23)

where *fn_referinta* is the normalized center-band frequency, *l* is the length of the coupled section normalized to the free-space wavelength and *h* is the height of the substrate.

The functions (19), (20), (22), (23) were employed to assess the elements of the four-port impedance matrix modelling the MIC coupled lines, equations (1)-(4), which were further employed to code functions that calculated the elements of the impedance matrices of SPS, equations (7)-(8), and SKPS (13)-(14).

Additional functions were defined for assessing the characteristic impedances and phase shifts of single/ isolated MIC transmission lines and also for calculating the input impedances of short-circuited MIC line stubs:

zsc(*eps_rel,z0,u_MIC,t,h,fn,fn_referinta,lsc*). (24)

where *u_MIC* is the width of the isolated MIC line normalized to the height of the substrate, and *lsc* is the length of the stub normalized to the free-space wavelength.

Thus, coding the functions for LPS impedance matrix elements became possible.

As soon as the elements of the impedance matrices were made available, coding functions for calculating the elements of the **S** matrices and the image impedances became straightforward.

As a conclusion, by implementing the analysis equations defined in references from [7] to [12], the conditions were met for generating all the functions required to calculate the parameters of interest. The said functions could be employed not only for analyzing the circuits of interest, but also for implementing the synthetizing algorithms required for the design of the circuits.

The accuracy of the functions implemented in the MATLAB library was assessed as satisfactory by comparing the results with those provided by the professional *transmission line analysis and synthesis software* included in Ansys CIRCUIT.

4. PHASE SHIFTER SYNTHESIS

The topologies of the three phase shifters under consideration are given in Fig. 4. The C-Sections modelled in section 2, are shown in the lower half of the three topologies. These sections should provide a 180-degree phase shift at the center frequency. In the upper halves of the topologies the so-called reference lines are shown. These lines should produce a 270 degrees phase shift at center frequency. The differential phase shift between the C-sections and the reference lines should be thus 90 degrees at center frequency.

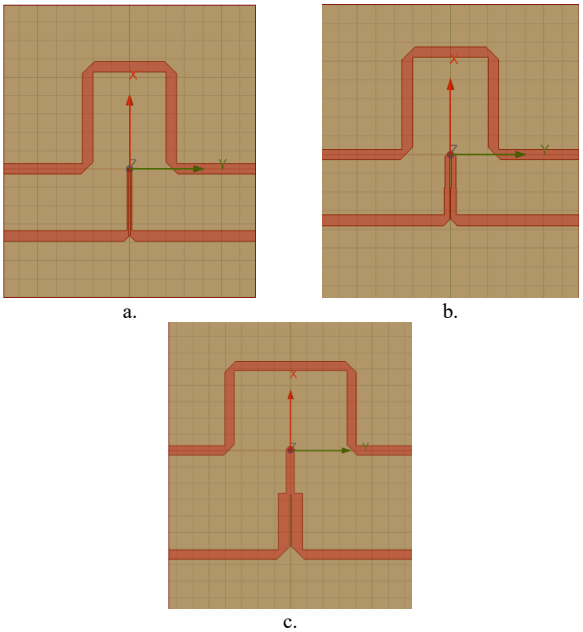

Fig. 4 - The topologies of the phase shifters synthetized in this article: a. Schiffman Phase Shifter (SPS); b. Schiek Phase Shifter (SKPS); c. Liu Phase Shifter (LPS).

To conduct the synthesis of the phase shifters, and due the intended destination of these circuits, the central frequency of f_0=2.4 GHz was chosen for the design. In addition, a FR4 substrate with 4.4 relative permittivity, 0.02 loss tangent

and 60 mil (1.524 mm) thick was employed in the modelling.

4.1 SHIFFMAN PHASE SHIFTER

A straightforward procedure for the synthesis of the SPS was tested by defining a differential phase shift error function which assesses the difference between the differential phase shift produced by the SPS and the value of 90 degrees, over the intended operation bandwidth of the phase shifter. By anticipating the fact that the differential phase shift error function of the SPS was S-shaped, and that the bandwidth of the SPS could be defined as the frequency interval between the outer nulls of the differential phase shift error function, the goals of achieving an octave bandwidth and good matching at center frequency were set.

Thus, the differential phase shift error function and the input reflection coefficient function (S_{11}) of the C-Section were defined in MATLAB based on (7), (8) and [6]. A genetic optimization algorithm was employed to synthesize the physical dimensions of the circuit while seeking to enforce nulls of the differential phase shift error function at the frequencies $f_0 - f_0/3$, f_0 and $f_0 + f_0/3$ (an octave) and a minimum of C-Sections' input reflection coefficient at f_0. In Fig. 5 and 6 the obtained results are centralized. To check and validate the physical dimensions of the circuit which were obtained because of the synthesis, an Ansys CIRCUIT model of the SPS was implemented, as shown in Fig. 7. In the figure, the simplified topology of the C-Section (A1) and the reference line are presented. The sizes of the lines in millimeters are also included. One can note that the dimensions of the circuit are physically achievable with ordinary etching equipment.

The results of performing the Ansys CIRCUIT simulation are also included in the plots presented in figures 5 and 6. It can be noted that the results produced by the MATLAB and Ansys CIRCUIT models are quite similar. The dissimilarities were produced by the fact that in this work, as mentioned before, a MATLAB implementation of the lossless transmission lines' analysis formulas was implemented.

In addition, the decision was made to produce an Ansys HFSS model of the SPS. The implemented circuit is shown in Fig. 4.a. The construction of the model in Ansys HFSS introduced an additional complication which consisted of the need to miter the corners produced by the 90 degrees transmission line junctions, as it can be seen in Fig. 4.a. The mitered corners proved instrumental in achieving satisfactory impedance matching of the C-Section and reference line.

On the other hand, mitering produces slight changes in the electrical lengths of the transmission lines which must be compensated for. Two optimization attempts were conducted using the tools available in Ansys HFSS. The first attempt sought to tune the SPS by intervening only on the miering and the physical lengths of the transmission lines.

The second attempt involved, in addition, an intervention on the width and gap of the coupled lines.

Even though the optimizations were carefully implemented, it can be noticed that no major differences were achieved between the HFSS results which were equivalent for all practical purposes. From a practical point of view, it is obvious that the MATLAB generated prototype of the SPS could be employed as a strong initial variant for developing more exact designs in a professional modeler such as Ansys HFSS.

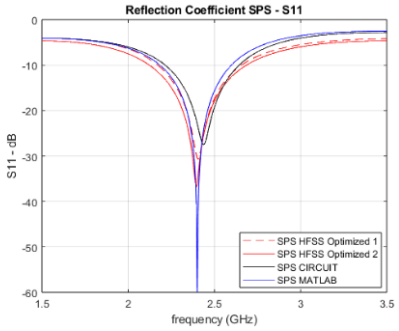

Fig. 5 – The input reflection coefficient (S_{11}) obtained with the SPS. The plots describe the results provided by the MATLAB tool which was developed, the ones obtained by implementing the SPS in Ansys CIRCUIT and two optimizations in Ansys HFSS.

As far as the results are concerned, the final bandwidth of the phase shifter (measured between the first and the last null of the S-shaped phase error plot) was slightly less than an octave (about 90% out of an octave).

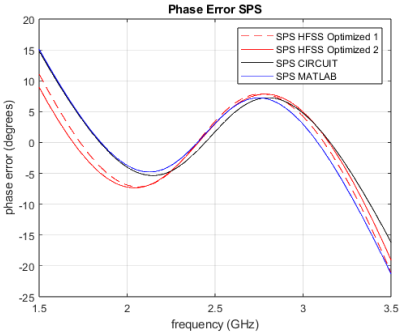

Fig. 6 – The differential phase shift error of the SPS. Similarly, as above, the results provided by MATLAB, Ansys CIRCUIT and Ansys HFSS are shown.

Using the central frequency as a reference, a 60% bandwidth was achieved. The maximum phase error within the defined bandwidth was less than 8 degrees which would be acceptable for most practical applications.

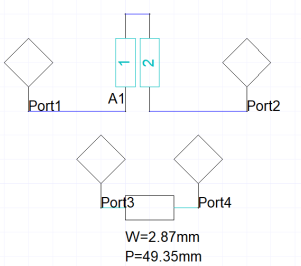

	Name	Value	Unit	Evaluated Value	Description
	W	0.34	mm	0.34mm	Conductor Width
	P	17.36	mm	17.36mm	Physical length
	SP	0.49	mm	0.49mm	spacing between cond...

Fig. 7 – The Ansys CIRCUIT model of the synthesized Schiffman Phase Shifter. The parameters of the coupled lines, as synthesized in MATLAB, are given in the table.

On the other hand, a serious limitation in the practical employment of the circuit was given by a relatively reduced matching bandwidth of only 24% (measured at -10 dB).

4.2 SCHIEK PHASE SHIFTER

In [3], Schiek and al. proposed a modified Schiffman phase shifter with improved matching over the entire useful bandwidth of the phase shifter. Schiek has also proposed an approximate synthesis algorithm for a microstrip phase shifter meeting the mentioned requirements. In the present approach, two simple goals were established for the MATLAB genetic optimization/ synthesis: the first objective was to extend the operation bandwidth of SKPS over an octave identically to the previous experiment; the second objective was to enforce impedance matching over the mentioned operation bandwidth.

Based on the results produced by the MATLAB code, Ansys Circuit and Ansys HFSS models were also implemented. The Ansys CIRCUIT model is given in Fig. 10, all the dimensions of the lines being included. While no interventions were made on the Ansys CIRCUIT model, it was necessary to carefully review the Ansys HFSS model due to its increased complexity. The results are compared in figures 8 and 9. One can note that, as far as the MATLAB and Ansys CIRCUIT were concerned, the results were well aligned with the stated objectives. The Ansys HFSS model required some additional fine-tuning by employing HFSS embedded optimization tools.

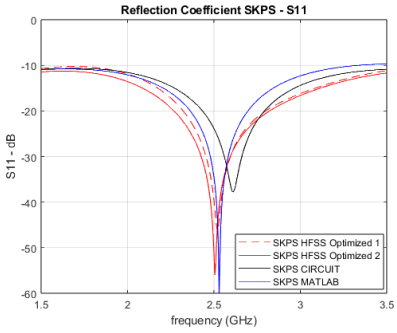

Fig. 8 – The input reflection coefficient (S_{11}) obtained with the SPS. The plots describe the results provided by the MATLAB tool which was developed, the ones obtained by implementing the SPS in Ansys CIRCUIT and two optimizations in Ansys HFSS

Of course, as the starting set of values in the Ansys HFSS optimizations, the MATLAB solution was employed. In the first optimization attempt, only the lengths of the transmission lines and the mitered corners were considered for optimization while in the second, the widths of the coupled lines and the spacing between the conductors of the coupled lines were also included.

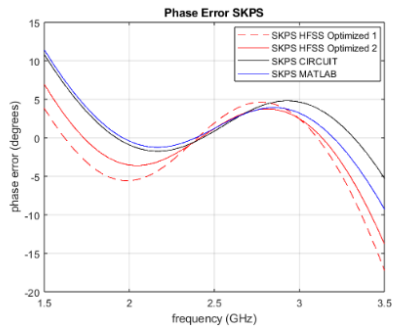

Fig. 9 – The differential phase shift error of the SKPS. The results provided by MATLAB, Ansys CIRCUIT and Ansys HFSS simulations are shown.

From the figures, the impedance matching was quite good irrespective of the optimization approach, while the control of the differential phase shift error function was more difficult. Nevertheless, the result of the second HFSS optimization is acceptable for practical implementation with a maximum phase error of 3.5 degrees over an operational bandwidth of 86% out of an octave and impedance matching over the entire mentioned bandwidth.

4.3 LIU PHASE SHIFTER

The last phase shifter under analysis was proposed by Liu et al. in [4]. The topology of the circuit is presented in Fig. 4.c. Equations (16), (17) the transformation tables in [6] and the phase shift produced by a 50 Ohm reference microstrip line were employed to develop a differential phase shift error function of the LPS.

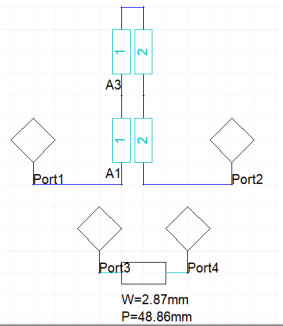

	Name	Value	Unit	Evaluated Value	Description
	W	0.94	mm	0.94mm	Conductor Width
	P	8.95	mm	8.95mm	Physical length
	SP	0.23	mm	0.23mm	spacing between cond...

	Name	Value	Unit	Evaluated Value	Description
	W	1.28	mm	1.28mm	Conductor Width
	P	8.17	mm	8.17mm	Physical length
	SP	0.15	mm	0.15mm	spacing between cond...

Fig. 10 – Ansys CIRCUIT model of the synthesized Schiek Phase Shifter. The parameters of the coupled lines, as calculated in MATLAB, are given in the tables (upper table for A3, lower table for A1).

In addition, to assess the matching of the modified C-Section, the input reflection coefficient S_{11} of the modified C-Section was implemented as a MATLAB function.

A MATLAB genetic optimization with constraints was tested by enforcing the phase condition (zero phase error) and matching at center frequency with the constraints of having good matching (reflection coefficient less than -15 dB) at the ends of phase shifter's bandwidth.

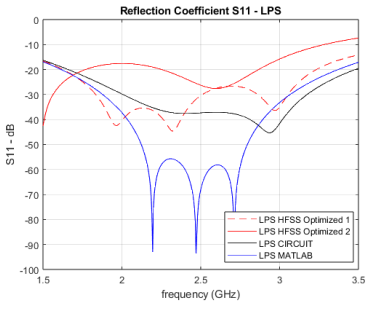

Fig. 11 – The input reflection coefficient (S_{11}) obtained with the LPS. The plots describe the results provided by the MATLAB tool, which was developed, the ones obtained by implementing the LPS in Ansys CIRCUIT and two optimizations in Ansys HFSS.

The results of the MATLAB optimization are given in Fig. 11 and 12. The figures also include the results provided by the Ansys CIRCUIT simulations when the results of the MATLAB synthesis were employed for building the Ansys CIRCUIT model shown in Fig. 13. The physical dimensions

of the circuit are indicated in the figure. As far as the phase error is concerned, it can be concluded that the results provided by the MATLAB and Ansys CIRCUIT are very similar. As far as matching is concerned, although the plots are not identical, the matching bandwidth is basically the same for both models.

Similarly to the previous subsections, two experiments were conducted with the goal of adapting the design to an Ansys HFSS model. The construction of the first Ansys HFSS model involved introducing the physical dimensions provided by the MATLAB and making the microstrip lines' lengths and the mitered corners tunable.

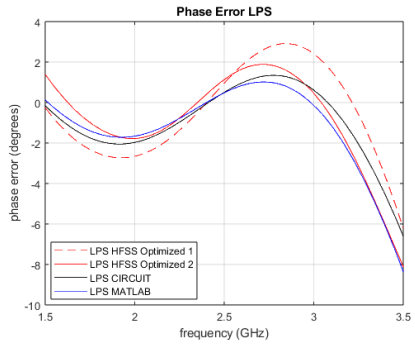

Fig. 12 – The differential phase shift error of the LPS. The results provided by MATLAB, Ansys CIRCUIT and Ansys HFSS simulations are shown.

By employing Ansys HFSS optimization tools, the results shown in Fig. 11 and 12 were obtained. One can note that a LPS bandwidth of over one octave was obtained with excellent matching. The maximum phase error within the operating bandwidth of the LPS was less than 3 degrees. The second experiment aimed at reducing the phase error under 2 degrees.

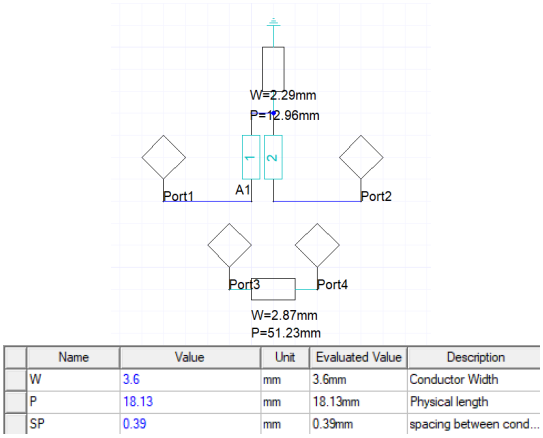

	Name	Value	Unit	Evaluated Value	Description
	W	3.6	mm	3.6mm	Conductor Width
	P	18.13	mm	18.13mm	Physical length
	SP	0.39	mm	0.39mm	spacing between cond...

Fig. 13 – Ansys CIRCUIT model of the synthesized Liu Phase Shifter. The parameters of the coupled line A1, as calculated in MATLAB, are provided in the table.

From Fig. 12 and Fig. 11, it is obvious that the main goal was achieved but, at a price. Thus, the bandwidth was reduced significantly and the matching although acceptable is much worse than in the previous experiments.

5. CONCLUSIONS

In this article, a workable approach to streamlining the prototyping of broadband 90 degrees microstrip phase shifters were demonstrated. Starting from a set of simple mathematical models proved in Section 2 and a library of microstrip line analysis equations, MATLAB functions for the required critical parameters of the phase shifters such as, differential phase error and input reflection coefficient, were coded. The functions were further employed in Section 4 for developing MATLAB genetic optimization algorithms adapted to three typical broadband phase shifters. Thus, a simplified approach to synthesizing the phase shifters of interest was demonstrated. The results were further employed for defining Ansys CIRCUIT and Ansys HFSS models of the same phase shifters which provided satisfactory results. The method can be easily adapted to other microstrip circuits provided the basic mathematical model of the circuit is properly deduced.

CREDIT AUTHORSHIP CONTRIBUTION STATEMENT

Laurențiu Iustin Buzincu: Responsible for developing the simplified mathematical models of the phase shifters, coding the MATLAB functions required for modeling the microstrip lines and the optimization of the phase shifters, implementing the Ansys Circuit and Ansys HFSS models of the phase shifters and conducting the simulations.
Ioan Nicolaescu: Responsible for identifying the phase shifters of interest for the present development, ensuring the theoretical coherence of the approach, defining the strategy of phase shifter synthesis and validation and contributing to the interpretation of the results obtained by synthesis and simulation.

Received on 21 March 2025

REFERENCES

1. E.M.T. Jones, J.T. Bolljahn, *Coupled-Strip-Transmission-Line Filters and Directional Couplers*, IRE Transactions on Microwave Theory and Techniques, **4**, *2*, pp. 75-81 (1956).
2. B.M. Schiffman, *A New Class of Broad-Band Microwave 90 Degree Phase Shifters*, IRE Transactions on Microwave Theory and Techniques, **6**, *2*, pp. 232-237 (1958).
3. B. Schiek, J. Kohler, *A Method for Broad-Band Matching of Microstrip Differential Phase Shifter*, IEEE Transactions on Microwave Theory and Techniques, **25**, *8*, pp. 666-671 (1977).
4. Q. Liu, H. Liu, Y. Liu, *Compact ultra-wideband 90° phase shifter using short-circuited stub and weak coupled line*, Electronics Letters, **50**, *20*, pp. 1454-1456 (2014).
5. A. Aloman, M. Poveda-Garcia, I. Nicolaescu, F. Popescu, L. Buzincu, *Circularly polarized periodic leaky-wave antenna based on a coaxial line with helical slot*, Rev. Roum. Sci. Techn.–Électrotechn. et Énerg., **70**, *1*, pp. 87-90 (2025).
6. D.A. Frickey, *Conversions between S, Z, Y, h, ABCD, and T parameters which are valid for complex source and load impedances*, IEEE Transactions on Microwave Theory and Techniques, **42**, *2*, pp. 205-211 (1994).
7. M. Nicolaescu, V. Croitoru, L. Tuță, *Transient analysis of a microstrip differential pair for high-speed printed circuit boards*, Rev. Roum. Sci. Techn. – Électrotechn. et Énerg., **67**, *2*, pp. 167-170 (2022).
8. M. Kirschning, R. H. Jansen, *Accurate model for effective dielectric constant of microstrip with validity up to millimetre-wave frequencies*, Electronics Letters, **18**, *6*, pp. 272-273 (1982).
9. M. Kirschning, R.H. Jansen, N.H.L. Koster, *Coupled Microstrip Parallel-Gap model for improved filter and coupler design*, Electronics Letters, **19**, *10*, pp. 377-379 (1983).
10. M. Kirschning, R.H. Jansen, *Accurate wide-range design equations for the frequency-dependent characteristic parallel coupled microstrip lines*, IEEE Transactions on Microwave Theory and Techniques, **32**, *1*, pp. 83-89 (1984).
11. T.G. Bryant, J.A. Weiss, *Parameters of microstrip transmission lines and of coupled pairs of microstrip lines*, IEEE Transactions on Microwave Theory and Techniques, **16**, *12*, pp. 1021-1027 (1968).
12. E. Hammerstad, O. Jensen, *Accurate models for microstrip computer-aided design*, IEEE MTT-S International Microwave Symposium Digest, pp. 407-409 (1980).